Pulsed Nuclear Magnetic Resonance: Spin Echoes

MIT Department of Physics
(Dated: February 8, 2011)

In this experiment, the phenomenon of Nuclear Magnetic Resonance(NMR) is used to determine the magnetic moments of the proton and the fluorine nucleus. The spin-lattice and spin-spin relaxation times are determined from the measurements of free-induction signals and spin echoes. The variation of relaxation constants with viscosity and concentration of paramagnetic ions is studied.

1. PREPARATORY QUESTIONS

1. Show that a particle with angular momentum $\vec{I}$ and magnetic moment $\vec{\mu} = \gamma\vec{I}$ placed in a uniform magnetic field $\vec{B_0}$ precesses with angular frequency $\vec{\omega_0}$ (called the Larmor angular frequency) that is independent of the angle between $\vec{\mu}$ and $\vec{B_0}$, given by

$$\vec{\omega_0} = -\gamma\vec{B_0} \equiv -(g\mu_N/\hbar)\vec{B_0}. \quad (1)$$

   Here g is the counterpart of the Landé g-factor in atomic spectroscopy and μ_N is the nuclear magneton, $e\hbar/2m_p$.

   For protons, $g = 5.58$, so $\gamma = 26.8 \times 10^3$ radians sec^{-1} gauss^{-1}, which corresponds to a Larmor frequency of 4.26 MHz at 1 kGauss magnetic field. Note that 1 Gauss = 10^{-4} Tesla.

2. Derive the classical expression for the potential energy of a magnetic dipole in a magnetic field.

3. According to quantum mechanics the component of angular momentum in a given direction, e.g. the direction of $\vec{B_0}$, is an integer or half-integer multiple of $\hbar$. Write an expression for the energies U_m of all the possible states of a nucleus with total angular momentum quantum number I in a magnetic field. Draw on a single diagram the variation of all U_m's with B_0 over the range 0 to 10,000 Gauss for the proton and the fluorine nucleus.

4. Show on the above diagrams the frequencies of photons which would cause transitions among the various levels at $B_0 = 1770$ Gauss. Confirm that the photon frequencies are the same as the corresponding Larmor frequencies.

5. The samples used in the NMR measurements contain very large numbers of the dipoles being studied. These interact with one another and are in thermal equilibrium at room temperature. The relative populations of their allowed energy states therefore follow the Boltzmann distribution, namely $N \propto e^{-E/kT}$. Calculate the fractional difference in the populations of the magnetic states of the proton, that is, $(n_+ - n_-)/(n_+ + n_-)$, in a sample at room temperature in a magnetic field of 1770 Gauss.

2. PROGRESS CHECK

By the end of your 2nd session in lab you should have a determination of the nuclear magnetic moment of fluorine. You should also have a preliminary value of T_2 for 100% glycerine.

3. THEORY OF NMR

The NMR method for measuring nuclear magnetic moments was conceived independently in the late 1940's by Felix Bloch and Edward Purcell [1–3]. Both investigators, applying somewhat different techniques, developed methods for determining the magnetic moments of nuclei in solid and liquid samples by measuring the frequencies of oscillating electromagnetic fields that induced transitions among their magnetic substates resulting in the transfer of energy between the sample and the measuring device. Although the amounts of energy transferred are extremely small, the fact that the energy transfer is a resonance phenomenon enabled it to be measured. Bloch and Purcell both irradiated their samples with a continuous wave (CW) of constant frequency while simultaneously sweeping the magnetic field through the resonance condition. CW methods are rarely used in modern NMR experiments. Radiofrequency (rf) energy is usually applied in the form of short bursts of radiation (pulsed NMR) and the effects of the induced energy level transitions are observed in the time between bursts. It is experimentally much easier to detect the extremely small effects of the transitions if this detection phase is separated in time from the rf burst phase. More importantly, as we shall see, it is much easier to sort out the various relaxation effects in pulse nmr experiments. The present experiment demonstrates the essential process common to all NMR techniques: the detection and interpretation of the effects of a known perturbation on a system of magnetic dipoles embedded in a solid or liquid. In addition, the effects of perturbations caused by the embedding material yield interesting information about the structure of the material.

3.1. Classical Motion of a Single Spin

One can describe the dynamics of a particle with spin in a magnetic field by drawing an analogy with a gyro-

scope in a gravitational field. The spin vector precesses about the field direction and then, as energy is transferred to or from the particle, the angle between its spin axis and the field axis gradually changes. This latter motion is called nutation.

The trouble with the gyroscope analogy would appear to be that an individual spin which obeys quantum mechanics cannot nutate continuously, since its projection on the field direction is quantized. Bloch, in 1956, proposed a vector model in which he showed that although nuclear spins obey quantum laws, the ensemble average taken over a large number of spins behaves like a classical system, obeying the familiar laws of classical mechanics. Thus one can gain significant insight by a classical analysis of a spinning rigid magnetized body in a magnetic field.

Following the discussion given by [4], we consider the motion of a nucleus with angular momentum $\vec{I}$ and magnetic moment $\vec{\mu} = \gamma\vec{I}$ in a magnetic field $\vec{B} = \vec{B_0} + \vec{B_1}$ composed of a strong steady component $B_0\hat{k}$ and a weak oscillating component $B_1 \sin(\omega t)\hat{\imath}$ perpendicular to B_0. Here $\hat{\imath}, \hat{\jmath}, \hat{k}$ are the unit vectors in the laboratory reference frame x, y, z. The quantity γ is called the gyromagnetic ratio. (In the present experiment, the strong steady field has a magnitude of several kiloGauss; the weak oscillating field is the field inside a small solenoid 2 cm long, wound with 10 turns, and connected to a crystal-controlled fixed-frequency generator and wide-band power amplifier producing an rf alternating current with a peak amplitude of ~ 1 mA at 5.00×10^6 Hz. A simple calculation will confirm that under such conditions $B_1 \ll B_0$). The equation of motion of the particle is

$$\frac{d\vec{I}}{dt} = \gamma\vec{I} \times \vec{B}. \tag{2}$$

If $B_1 = 0$, the motion in a reference frame fixed in the laboratory is a rapid precession of the angular momentum about the direction of $\vec{B_0}$ (the z-axis) with the Larmor precession frequency γB_0, as shown in one of the preparatory questions. To understand the perturbing effects of the small-amplitude oscillating field on the motion we first represent it as the vector sum $\vec{B_1} = \vec{B_r} + \vec{B_l}$ of two counter-rotating circularly polarized components given by the equations

$$\begin{aligned} \vec{B_r} &= \tfrac{1}{2}(B_1 \cos\omega t\ \hat{\imath} + B_1 \sin\omega t\ \hat{\jmath}) \\ \vec{B_l} &= \tfrac{1}{2}(B_1 \cos\omega t\ \hat{\imath} - B_1 \sin\omega t\ \hat{\jmath}), \end{aligned} \tag{3}$$

where the subscript l denotes the component rotating in the direction of rapid precession (the proton precesses in the left hand direction as can be seen by solving Eq. 2), and r denotes the component rotating in the opposite direction.

Next we consider the situation from the point of view of an observer in a reference frame x', y', z' rotating in the direction of precession with angular velocity ω and unit vectors:

$$\begin{aligned} \hat{\imath}' &= \cos\omega t\ \hat{\imath} + \sin\omega t\ \hat{\jmath} \\ \hat{\jmath}' &= -\sin\omega t\ \hat{\imath} + \cos\omega t\ \hat{\jmath} \\ \hat{k}' &= \hat{k}. \end{aligned} \tag{4}$$

In this rotating frame $\vec{B_r}$ is a constant vector $(B_1/2)\hat{\imath}'$, $\vec{B_l}$ is rotating with angular velocity -2ω, and the rapid precession will have angular frequency $\gamma(B_0 - \omega/\gamma)$, as though the particle were in a field whose z-component is B_0 plus a fictitious field in the opposite direction of magnitude ω/γ. Suppose now that ω is adjusted so that $\omega = \gamma B_0$. Then the rapid precession will vanish, i.e. its frequency in the rotating frame will be zero, and the particle will precess slowly about the direction of the steady field $(B_1/2)\hat{\imath}'$ with angular velocity $\gamma B_1/2$, with only a tiny flutter averaging to zero due to the counter-rotating component. If $\vec{I}$ is initially parallel to B_0, then in time $\pi/(\gamma B_1)$ the spin direction will precess by 90°, putting $\vec{I}$ in the $x'y'$ plane, perpendicular to B_0. If the oscillating field is now turned off, the particle will be left with its magnetic moment in the $x'y'$ plane and, from the point of view of an observer in the laboratory frame, it will be rotating in the xy-plane with angular frequency γB_0 about the z-direction.

3.2. Dynamics of an Ensemble of Spins

According to the Bloch theorem, this classical treatment of a single magnetized spinning body is actually valid for an ensemble of quantized magnetic moments.

Consider such a sample containing protons placed between the poles of the magnet. According to the Boltzmann distribution law, if the sample is in thermal equilibrium at temperature T, then the ratio of the number of protons n_+ with z components of spin up to the number with z components down is

$$n_+/n_- = e^{(-E_+ + E_-)/kT} = e^{\mu_p B_0/kT}, \tag{5}$$

where μ_p is the magnetic moment of the proton. At room temperature in a field of several kilogauss this ratio is only slightly greater than one, which means that the magnetization due to alignment of the proton moments in the z-direction is very slight.

Now, if the ensemble is rotated 90° by application of an rf field under the conditions described above for the correct amount of time (a "90° rf burst"), then the nuclear magnetization will end up in the plane perpendicular to B_0 and precess with angular velocity γB_0 about the z direction. The precessing magnetization creates an alternating magnetic flux in the solenoid which, according to Faraday's law, induces an rf voltage. This rf voltage can be readily detected after the rf burst has been terminated, thereby proving that the resonance condition was achieved and that the applied frequency was equal to or very close to the precession frequency of the protons. Knowledge of the field strength and the resonance

frequency allows the determination of the gyromagnetic ratio of the proton, which is a measurement of fundamental importance in nuclear physics.

To detect the nuclear-induced rf signal of angular frequency γB_0 that appears across the terminals of the solenoid immediately after the 90° rf burst, it is mixed with a steady signal of frequency ω from the fixed oscillator to produce a beat signal of comparatively low frequency $|\gamma B_0 - \omega|$ which can be observed directly on an oscilloscope. The 90° rotation of magnetization still works even if ω is slightly off resonance.

However, the precession of spins in the transverse plane does not last forever. It decays because of three distinct effects:

1. The field of the magnet is not perfectly uniform so that the protons in different parts of the sample precess at slightly different frequencies and get out of phase with one another, thereby gradually decreasing the net magnetization of the sample. This effect, although physically the least interesting, is always the dominant effect.

2. Protons in any given substance are generally located in several different molecular environments in each of which the precession frequency will be perturbed in a slightly different amount by magnetic dipole interactions. As in 1) the result is a gradual loss of phase coherence and a decay of the resultant magnetization.

3. Electromagnetic interactions between the protons and the surrounding particles cause transitions between the spin up and spin down states whose coherent combination is manifested as magnetization rotating in the xy-plane. The result is a gradual decay of these coherent combinations and a return to the state of thermal equilibrium in which the magnetization is in the z-direction and therefore no longer capable of inducing a signal in the solenoid.

The oscillatory induced signal modulated by a decaying exponential (Figure 1) is referred as the Free Induction Decay (FID.) An excellent reference describing these relaxation effects is given in [5] and is available from the Junior Lab e-library.

3.3. Spin-Lattice Relaxation Time, T_1

Application of rf pulses and the consequent rotation of the spins from the z-axis to the xy-plane is a disruption of the thermal equilibrium of the spins. Effect number 3 described above is called thermal relaxation, that is, the approach to thermal equilibrium after being disturbed by the rf pulse.

How fast the spins regain equilibrium is a measure of the coupling of the protons to their environment. The approach to equilibrium is exponential and is characterized

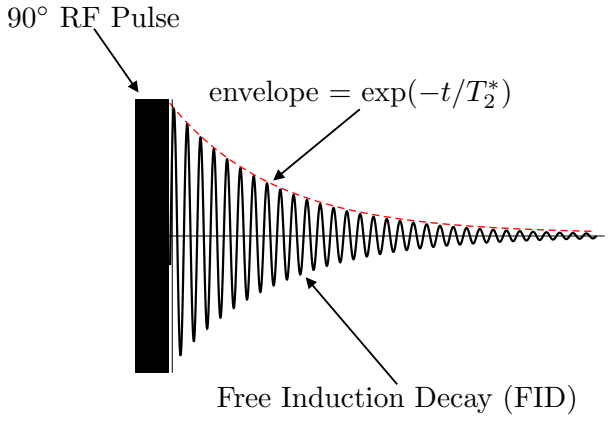

FIG. 1: The Free Induction Decay.

by a time constant denoted by T_1, called the spin-lattice or the longitudinal relaxation time. We can write

$$M_z(t) = M_z^{eq} + (M_z(0) - M_z^{eq})e^{-t/T_1},$$

where $M_z(t)$ is the z-magnetization at time t and M_z^{eq} is the value of z-magnetization at thermal equilibrium. The process of thermal relaxation is governed by the ease with which the nuclei are able to exchange energy with their surroundings. Transfer of energy from the spins to the lattice requires that there be a fluctuating magnetic field with Fourier components vibrating near the Larmor precession frequency in order to induce NMR transitions. The field originates from magnetic dipoles which are in thermal agitation.

3.4. Spin-Spin Relaxation Time, T_2

The time constant T_1 described in the previous section measures the regaining of longitudinal magnetization. However, there is another process that happens. With the passage of time after the rf pulse puts the spins in the transverse plane, the magnetic moments interact with one another and lose their phase coherence in the xy-plane (this is effect number 2 described above). This loss of transverse magnetization is characterized by the time constant T_2, called the spin-spin or the transverse relaxation time.

T_2^* is the name given to the observed value of the decay constant. This observed time constant consists of two components

$$1/T_2^* = 1/T_2 + \gamma \Delta H_0, \tag{6}$$

where T_2 is the spin-spin, or the transverse relaxation time and ΔH_0 is the inhomogeneity of the magnetic field over the sample volume. The second term on the right is always larger than $1/T_2$ and is sometimes referred to in the literature as $1/T_2'$.

The measurement of T_2 is the basis for the powerful method of pulsed NMR chemical analysis based on measurement of the various perturbed precession frequencies

due to the various locations of the protons within the molecule. Given the spectrum of these frequencies for a new complex organic compound, an expert can practically write out the chemical formula.

In many cases, the same physical mechanisms determine T_1 and T_2 so that they are equal. The cases of interest are those where there are additional mechanisms for spin-spin relaxation such that T_2 is shorter than T_1. After a 90° pulse all phase coherence may be lost before any substantial z-magnetization is recovered. The transverse magnetization, and thus also the rf voltage induced in the sample coil, fall off as the phase coherence is lost. The dominant effect of magnet inhomogeneity, which could be fatal for such precision measurements, can be virtually eliminated by the remarkable invention of Hahn who discovered the phenomenon of "spin echoes" [6, 7]. Fig. 1 shows an FID (Free Induction Decay).

4. MEASUREMENT TECHNIQUES

4.1. The Measurement of T_2: Spin Echoes

To see how a spin echo is produced, consider a typical sample which has an enormous number of protons, of the order of 10^{23}. They can be divided into millions of ensembles, each one of which consists of a still enormous number of protons in a region where the external field has values within a very narrow range. Each ensemble will have a certain net magnetization which contributes to the total magnetization, but each such magnetization will precess with a slightly different frequency and therefore gradually get out of phase with respect to the others.

Suppose that after a sufficiently long time interval τ, a second transverse rf burst of double duration, i.e. a 180° burst, is applied to the sample.

The magnetization of each ensemble will be flipped by 180° about the direction of the applied pulse. This puts the magnetization back in the xy-plane where it will resume its precession motion. But now the accumulated phase differences between the various ensembles are all precisely reversed. Those that were ahead of the average are now behind by the same amount, and as the precession proceeds, the dephasing of the ensembles is gradually reversed. After precisely the same time interval τ all the ensembles are back in phase, the total magnetization reaches a maximum, and a "spin echo" signal is induced in the solenoid.

The amplitude of the echo is usually smaller than that of the original FID. There will be some loss in magnitude of the magnetization due to thermal relaxation and the effects of random fluctuations in the local fields that perturb the precession of the nuclear moments and it is precisely the relaxation time of this loss that we wish to measure. The spin-echo method enables one to eliminate the otherwise dominant effects of the nonuniformity of the magnetic field. If the two-pulse sequence is repeated for several different values of τ, the height of the echo should vary as $\exp(-t/T_2)$.

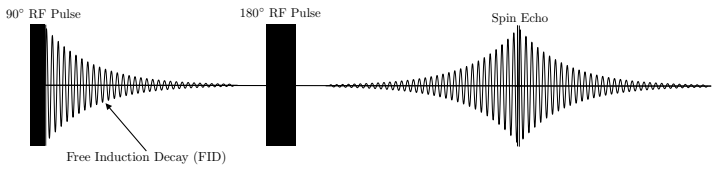

FIG. 2: The NMR signal observed when the applied rf frequency is offset slightly from the Larmor frequency. The fast oscillations corresponds to the beat between the two frequencies.

A necessary assumption implied in the spin-echo technique is that a particular spin feels the same constant magnetic field before and after the "refocusing" 180° pulse. If, because of Brownian motion, a spin has diffused to a different region of magnetic field before the echo, then that spin will not be refocused by the 180° pulse. This is often the case for non-viscous liquids and will result in a decay of echoes which is not quite exponential and somewhat faster than that observed in viscous liquids. The **Carr-Purcell** technique, described in [8, 9] and summarized below, elegantly addresses this difficulty. The section of this lab guide entitled "measurements" will ask you to take data to measure the apparent T_2 for two samples (e.g. a viscous sample such as glycerine and a non-viscous one such as H_2O containing Fe^{3+}) to compare with later measurements taken from the same samples by the Carr-Purcell technique.

4.2. The Measurement of T_1

We describe three methods of measuring T_1.

4.2.1. $90° - 90°$

As mentioned above, the spin-lattice relaxation time (T_1) can be measured by examining the time dependence of the z-magnetization after equilibrium is disturbed. This can be done by saturating the spins with a 90° pulse, so that the z magnetization is zero. Immediately after the first pulse one should be able to observe a free induction decay (as in Fig.1) whose amplitude is proportional to the z-magnetization just before the pulse. One then waits a measured amount of time, τ, so that some magnetization has been reestablished, and then applies a 90° pulse to the recovering system. The second 90° pulse will rotate any z magnetization into the xy plane, where it will produce a FID signal proportional to the recovered magnitude it had just before the second pulse. If the two-pulse sequence is repeated for different values of τ, the amplitude of the FID as a function of t will give the value of T_1.

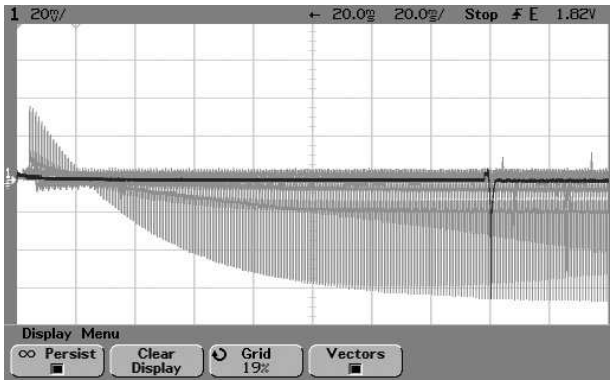

FIG. 3: An example data set using the "Three-Pulse" technique with the oscilloscope set to infinite-persist.

4.2.2. $180^\circ - 90^\circ$

Another sequence, the $180^\circ - \tau - 90^\circ$, is also used. A 180° pulse is applied to the equilibrium system, causing the population of the states to be precisely inverted, and thus leaving the xy-magnetization at zero. In this case, there should be little or no FID immediately after the first pulse. The system is then allowed to approach equilibrium for a specified delay, after which a 90° pulse is applied to rotate the partially recovered z-magnetization into the xy-plane. The magnitude of the FID gives a measure of the size of the magnetization, which can be plotted against the delay to give the exponential time constant. In this case, the magnetization actually reverses, going through zero at time $T_1 \ln 2$.

4.2.3. $180^\circ - \tau - 90^\circ\ 180^\circ$

It was mentioned earlier that it is experimentally much easier to detect the extremely small effects of transitions if they are separated in time from the multi-watt rf bursts. Unfortunately, the usual "Inversion Recovery" method requires observation of the FID immediately after the second rf pulse. This problem was addressed several years ago by two Junior Lab students[1], who proposed the "Three-Pulse" sequence [10]. See Figure 3 for a sample data set using this technique.

The first pulse (180°) inverts the population along the z axis as in the normal Inversion-Recovery method. After a delay of τ, the second and third pulses can be understood as a normal $180^\circ - \tau - 90^\circ$ sequence, which is used to measure the fraction of spins which are in the $|+z\rangle$ state at the moment that the pulses are applied. The time between the second and third pulses is kept small to minimize T_2 effects. The amplitude of the echo is therefore related to the amount of T_1 decay (or recovery) for a given value of τ. Varying τ will have the form $A(1 - 2\exp(-\tau/T_1))$.

The three experiments mentioned so far, (i.e. the spin-echo, the $90^\circ - 90^\circ$ and the $180^\circ - 90^\circ$ sequences) have each been performed successfully many times in this lab. However, each has its intrinsic difficulties leading to various modifications which will be discussed.

5. EXPERIMENTAL APPARATUS

This experiment uses a permanent magnet whose field is ~ 1770 Gauss (0.177 Tesla). Care should be taken to avoid bringing any magnetizable material (such as iron or steel) near the magnet as this may be pulled in and damage the magnet.

The experimental apparatus, shown in Figure 4 consists of a gated rf pulse generator with variable pulse widths and spacings, a probe circuit that delivers rf power to the sample and picks up the signal from the sample, a preamp that amplifies the signal, and a phase detector which outputs an audio signal whose frequency corresponds to the difference between the Larmor frequency and the frequency of the signal generator. Details of how to design and build NMR probes can be found in [11].

The rf pulse generating system is made up of a 15 MHz frequency synthesizer (Agilent 33120A), a digital pulse programmer based on a STAMP micro-controller, a double-balanced mixer used as an rf switch (Mini-Circuits ZAS-3), a variable attenuator, and an rf power amplifier capable of 2 watts output.

The frequency synthesizer feeds a +10dBm rf sine wave to the power splitter. The power splitter keeps all impedances appropriately matched while feeding one half of the rf power to a double-balanced mixer (DBM) used as a gate for the rf. The other half is used as a reference signal in the phase detector. The gate is opened and closed by TTL pulses provided by the digital pulse programmer. After the switching stage, the rf pulses pass into a constant-gain (+33 dBm) rf power amplifier. The power amplifier feeds the amplified pulsed rf into the probe circuit.

The signal out of the sample, as well as a considerable amount of leakage during pulses, comes from the probe circuit, and is amplified by a sensitive preamp (Tron-Tech W110F). The signal then goes into a phase detector (Mini-Circuits ZRPD-1), where it is mixed with the reference signal coming out of the other port of the power splitter. Since the NMR signal is, in general, not precisely at the frequency of the transmitter, when the two signals are mixed, a signal is produced at the difference frequency of the resonance signal and the applied rf. Since we are looking at NMR signals in the vicinity of 1-8 MHz, mixing this down to a lower frequency makes it easier to see the structure of the signal.

[1] Both of these students, Rahul Sarpeshkar and Isaac Chuang, are now M.I.T. professors. Creativity in Junior Lab is one indicator of future success in science!

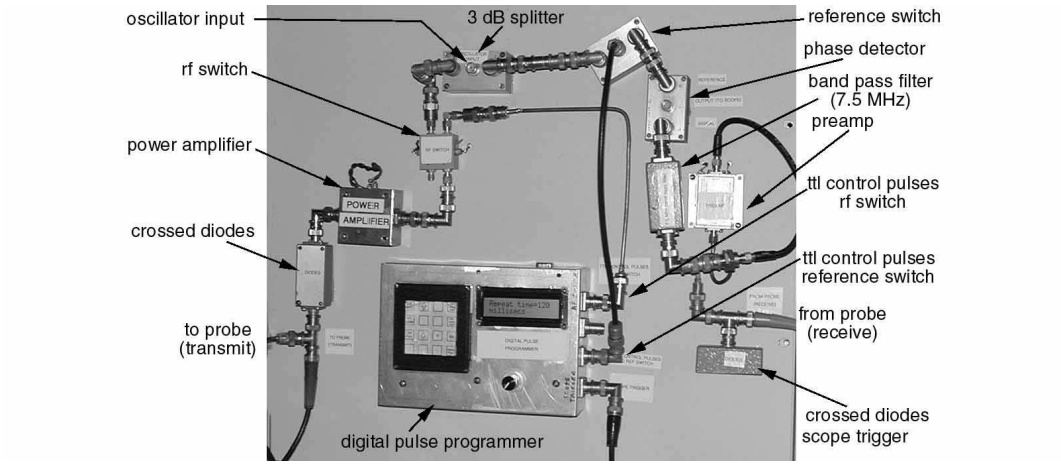

FIG. 4: The Experimental Setup. The magnet and the probe circuit are not shown

5.1. The probe circuit

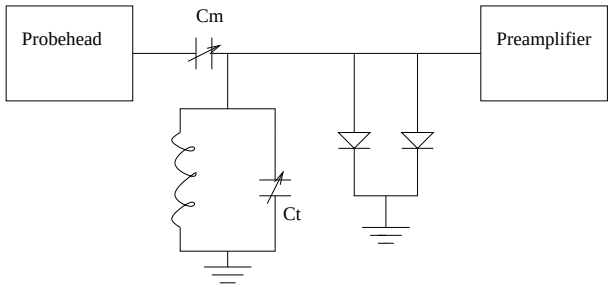

FIG. 5: Schematic of the probehead circuit.

The probe circuit is a tuned LC circuit, impedance matched to 50 ohms at the resonant frequency for efficient power transmission to the sample. The inductor L in the circuit is the sample coil, a ten turn coil of #18 copper wire wound to accommodate a standard 10mm NMR sample tube. The coil is connected to ground at each end through tunable capacitors C_m and C_t, to allow frequency and impedance matching. Power in and signal out pass through the same point on the resonant circuit, so that both the power amplifier and the signal preamp have a properly matched load. Between the power amplifier and the sample is a pair of crossed diodes, in series with the probe circuit from the point of view of the power amplifier. By becoming non-conducting at low applied voltages, these serve to isolate the probe circuit and preamp from the power amplifier between pulses, reducing the problems associated with power amplifier noise. The crossed diodes however, will pass the high rf voltages that arrive when the transmitter is on. The signal out of the probe circuit passes through a quarter-wavelength line to reach another pair of grounded crossed diodes at the input of the preamp. The diodes short the preamp end of the cable when the transmitter is on, causing that end of the cable to act like a short circuit. This helps to protect the delicate preamp from the high rf power put out by the power amplifier. Any quarter-wave transmission line transforms impedance according to the following relation:

$$Z_{in} = Z_0^2/Z_{out} \tag{7}$$

where Z_0 is the characteristic impedance of the line.

Therefore during the rf pulse, the preamp circuit with the quarter-wave line looks like an open circuit to the probe and does not load it down. Between pulses, the voltage across the diodes is too small to turn them on, and they act like an open circuit, allowing the small NMR signal to pass undiminished to the preamp.

6. EXPERIMENTAL PROCEDURE

Although it is the policy in Junior Lab to discourage the use of pre-wired experiments, there are two reasons why the present set-up should not be (lightly) changed. Several of the components, particularly the double-balanced mixers (DBM) and the low-level TRONTECH pre-amplifier, are easily damaged if the rf power level they are exposed to exceeds their specified limit. Furthermore, the lengths of some of the cables have been specifically selected to fix the relative phase relationship of different signals.

Most of the controls that you will manipulate are on the digital pulse programmer, the oscilloscope or the function generator. The keypad of the Digital Pulse Programmer is shown in Figure 6. Press any of the four buttons on the right to select a parameter (First Pulse Width (PW1), Second Pulse Width (PW2), Tau (τ), or Repeat Time). Then use the arrow buttons to set the corresponding time for that parameter. The default times are: PW1 = 24μs, PW2 = 48μs, τ = 2ms, and Repeat Time = 100ms. The top two buttons on the left determine whether a two-pulse sequence occurs only once

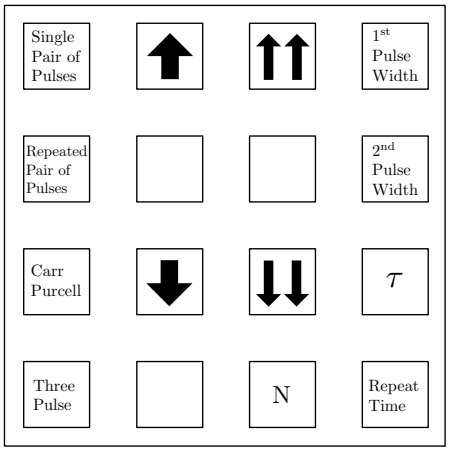

FIG. 6: The Pulse Programmer Interface.

(the Single Pair of Pulses buttom), or repeats continuously (the Repeated Pairs of Pulses button) with a pause between sequences of a length set by the Repeat Time parameter. The third button, labeled "Carr-Purcell," will create a series of pulses corresponding to the Carr-Purcell technique described in Section 6.3. Finally, the fourth button, "Three Pulse," outputs 180° $-\tau-$ 90° 180° pulses for a measurement.

Set the delay, τ, to the minimum position and observe the amplified rf pulses from the port marked "transmitter" on channel 2 of the oscilloscope. The pulses should be approximately 20-30 volts peak-to-peak. Choose the slowest possible sweep speed; this will enable both pulses to be viewed simultaneously. A good starting pair of pulse-widths might be 24 μs and 48 μs, corresponding to approximately 90° and 180°. Now switch to channel 1, which displays the output of the phase detector (through the low-pass filter). Incidentally, there is another low-pass filter which is part of the scope itself. On the Tektronix analog scope there is a button marked "BW limit 20 MHz", which limits the allowed bandwidth. This button should be pressed in (active). On the HP digital scope the BW limit is set by one of the soft keys. On an Agilent scope, this is set in the channel 1 or channel 2 menu. Set the y-sensitivity to about 10 mV/div at first. Channel 1 will display the NMR signal. Place the glycerine vial in the probe and place the probe in the magnet. Now the fun begins!

Refer to Figure 2, which is a highly stylized version of the signals you might obtain. The form of the voltage displayed during the two bursts is unimportant. You will be focusing your attention on the FID signals that appear after each burst, and on the echo. For five or ten microseconds after the rf pulse the amplifier is still in the recovery phase, so this part of the signal should be ignored.

6.1. Free Induction Decay (FID)

As mentioned above, the oscillations following the first pulse represent a beat between the applied rf frequency and the Larmor frequency. Since the latter is proportional to B_0, you should see high-frequency oscillations as you raise ω from below the resonance condition. They will spread out in time, pass through a zero-beat condition and then begin to increase in frequency again as the field continues to increase. These oscillations with their exponentially decaying envelope is referred to as the Free Induction Decay (FID).

6.2. Setting Pulse Widths

It is sometimes easiest to set the pulse widths with the magnetic field slightly off resonance so that the FID is well displayed. The size of the FID should be maximum after a 90° or 270° pulse, minimum or zero after a 180° pulse. It is usually easiest to set the pulse-width to 180° by minimizing the FID. Then, if you want a 90° pulse, halve the pulse-width.

You have four or more degrees of freedom, including the widths of each of the two pulses, the delay between the pulses, and the frequency of the applied current. Experiment with all of them. Look for FID's; vary the FID so that you get varying amounts of oscillations (beats), and try to explain the beats. Once you find oscillatory FID's, move the probe slightly between the pole pieces of the magnet in a direction perpendicular to the magnetic field. Explain the changes you see. Use these changes to find the most homogeneous position in the field, then leave the probe there for the remainder of the experiment. Measure T_2^*. Using various combinations of 90° and 180° rf pulses, obtain data from which you can determine T_1 and T_2 in several samples (see Section 7.)

6.3. The Carr-Purcell Experiment

The Carr-Purcell experiment is a technique used to measure T_2. As mentioned above, if diffusion causes nuclei to move from one point of an inhomogeneous magnetic field to another in a time less than 2τ, the echo amplitude is reduced. It can be shown that the echo amplitude for a pulse separation τ is

$$E(2\tau) = E(0)\exp\left[-\frac{2\tau}{T_2} - \frac{2}{3}\gamma^2 G^2 D\tau^3\right], \qquad (8)$$

where G is the gradient of the inhomogeneous field and D is the diffusion constant. Because of the τ^3 dependence, the effects of diffusion are pronounced for large values of t and thus affect the measurement of long T_2's. Carr and Purcell [8] introduced a pulse sequence which can be described as follows: $\pi/2, \tau, \pi, 2\tau, \pi, 2\tau, \pi, 2\tau...$ (i.e. 90 deg pulse at time 0, followed by 180 deg pulses at times

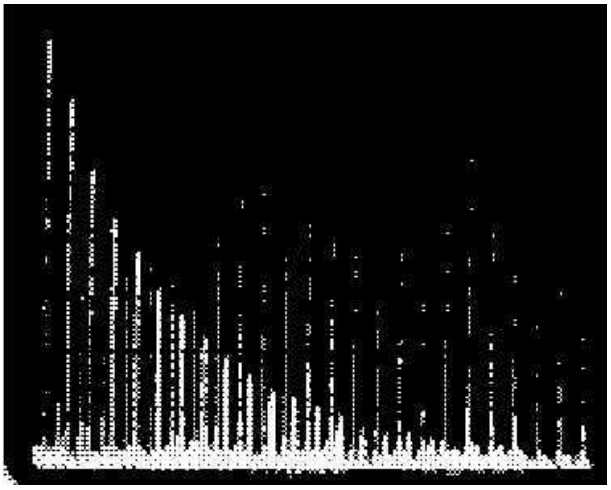

FIG. 7: The Carr-Purcell pulse and echo sequence

$\tau, 3\tau, 5\tau$, etc.) Echoes will be observed at times $2\tau, 4\tau, 6\tau$, etc.

When you are ready to do a Carr-Purcell, set up the pulse width and magnetic field first with a two-pulse spin echo and then switch to the Carr-Purcell mode using the pulse programmer. The scope readout should resemble Figure 7.

7. MEASUREMENTS

7.1. Magnetic Moments of Hydrogen and Fluorine

With this apparatus, we can measure the magnetic moments of two nuclei: the proton ^1H and the Fluorine nucleus ^{19}F. One of the strongest signals you can detect is due to hydrogen in glycerine. Once you have obtained a good resonance, remove the sample and replace it with the transverse probe of the Hall Gaussmeter. From the magnetic field strength ($\sim$ 1770 Gauss) and the measured frequency you can calculate the magnetic moment. Repeat the measurement for fluorine using the trifluoric acetic acid sample or the hexafluorobenzene (you may wish to consult the CRC or another source to get an idea of what resonant frequency you are looking for). The former is a strong acid and should be handled with extreme care. Before looking for the fluorine resonance, move the knob on the probe circuit in the magnet to point to "F". Also note that the T_1 relaxation time for our fluorine sample is long and if you use the default (100 ms) repetition rate of the pulse sequence, the observed signal will be small! Finally, be creative with the pulse programmer. For example, by setting pw2 = 1μs you can effectively create a one pulse sequence.

7.2. Relaxation Constants for Water

In the case of water, the relaxation times (T_1 equals T_2 for most non-viscous liquids) are of the order of several seconds. The measurement of T_2 is quite difficult but the equivalent measurement of T_1 can be done as follows:

Set up a $90° - 180°$ echo sequence with the shortest possible delay between pulses. As mentioned above, one must usually wait at least 5 times T_1 between successive repeats of this pulse sequence to allow sufficient time for equilibrium to be re-established. If less time is taken, the echo signal is diminished. Taking advantage of this fact, one can vary the repeat rate and plot the echo height against the repeat time. For times less than about 3 sec, you can read this repeat time from the small numerical display on the scope (push the button marked "per"). For slower rates switch to the manual ("one-shot") mode and use your watch to wait a specified amount of time in between pulses. Repeat the measurement for both tap-water and distilled water.

The first measurements of T_1 in distilled water stood for about thirty years. Since then careful measurements have produced a number which is about 50% higher. The difference is due to the effect of dissolved oxygen in the water (O_2 is paramagnetic). As an optional experiment, you might try to carefully remove the dissolved oxygen from a sample of distilled water. Bubbling pure nitrogen through the water will work as will other methods in the literature. A challenging question which you might discuss in your oral examination is why O_2 is paramagnetic while N_2 is diamagnetic.

7.3. Effects of Paramagnetic Ions

An extremely small amount of any substance with unpaired electron spins has a very dramatic effect of reducing T_1. There is a bottle of $FeCl_3.6H_20$ in the lab. The standard starting solution has a molarity of 0.166M corresponding to approximately 10^{20} Fe^{+++} ions/cc. There are 10 molar dilutions made from the standard solution with which measurements of both T_1 and T_2 should be taken. Repeat your measurements across the dilutions several times to ensure accuracy and precision. Plot the relaxation times versus concentration on a log-log scale.

7.4. Effect of Viscosity

It has been shown that the major contribution to both T_1 and T_2 processes comes from the fluctuating dipolar fields of other nuclear (and unpaired electron) spins in the immediate region. Only those fluctuations which have a sizeable Fourier component at the Larmor frequency can affect T_1, but spin-spin relaxation is also sensitive to fluctuations near zero frequency. It is for this reason that viscous liquids (whose fluctuations have a sizeable low-frequency component) exhibit a T_2 less than

Viscosity of Aqueous Glycerine Solutions in Centipoises/mPa s

Glycerine per cent weight	Temperature (° C)										
	0	10	20	30	40	50	60	70	80	90	100
0 [1]	1.792	1.308	1.005	0.8007	0.6560	0.5494	0.4688	0.4061	0.3565	0.3165	0.2838
10	2.44	1.74	1.31	1.03	0.826	0.680	0.575	0.500	–	–	–
20	3.44	2.41	1.76	1.35	1.07	0.879	0.731	0.635	–	–	–
30	5.14	3.49	2.50	1.87	1.46	1.16	0.956	0.816	0.690	–	–
40	8.25	5.37	3.72	2.72	2.07	1.62	1.30	1.09	0.918	0.763	0.668
50	14.6	9.01	6.00	4.21	3.10	2.37	1.86	1.53	1.25	1.05	0.910
60	29.9	17.4	10.8	7.19	5.08	3.76	2.85	2.29	1.84	1.52	1.28
65	45.7	25.3	15.2	9.85	6.80	4.89	3.66	2.91	2.28	1.86	1.55
67	55.5	29.9	17.7	11.3	7.73	5.50	4.09	3.23	2.50	2.03	1.68
70	76	38.8	22.5	14.1	9.40	6.61	4.86	3.78	2.90	2.34	1.93
75	132	65.2	35.5	21.2	13.6	9.25	6.61	5.01	3.80	3.00	2.43
80	255	116	60.1	33.9	20.8	13.6	9.42	6.94	5.13	4.03	3.18
85	540	223	109	58	33.5	21.2	14.2	10.0	7.28	5.52	4.24
90	1310	498	219	109	60.0	35.5	22.5	15.5	11.0	7.93	6.00
91	1590	592	259	127	68.1	39.8	25.1	17.1	11.9	8.62	6.40
92	1950	729	310	147	78.3	44.8	28.0	19.0	13.1	9.46	6.82
93	2400	860	367	172	89	51.5	31.6	21.2	14.4	10.3	7.54
94	2930	1040	437	202	105	58.4	35.4	23.6	15.8	11.2	8.19
95	3690	1270	523	237	121	67.0	39.9	26.4	17.5	12.4	9.08
96	4600	1580	624	281	142	77.8	45.4	29.7	19.6	13.6	10.1
97	5770	1950	765	340	166	88.9	51.9	33.6	21.9	15.1	10.9
98	7370	2460	939	409	196	104	59.8	38.5	24.8	17.0	12.2
99	9420	3090	1150	500	235	122	69.1	43.6	27.8	19.0	13.3
100	12070	3900	1410	612	284	142	81.3	50.6	31.9	21.3	14.8

[1] Viscosity of water taken from "Properties of Ordinary Water-Substance." N.E. Dorsey, p. 184. New York (1940)

FIG. 8: The viscocity of water-glycerine mixtures. Taken from http://www.dow.com/glycerine/resources/table18.htm

T_1. You will find a series of samples of glycerine-water mixtures in different ratios. Each will be marked with its viscosity[2] Measure T_2 by the Carr-Purcell method and T_1 by the $180° - 90°$ method, the three-pulse method or the method suggested in Subsection 7.2. With the aid of Figure 8, compare your results with those found in the extraordinary thesis of Bloembergen [12] started in the year that NMR was discovered.

[2] Recall that viscosity of a fluid, designated η is defined as the ratio for the shear stress placed on a fluid to the resultant strain rate. $\eta = \frac{F/A}{v/l}$ From the units, one can see that the SI units must be $1\frac{Ns}{m^2} = 1Pa\ s$ It is much more common however to see the corresponding 'cgs' unit 1 poise $= 1\frac{dyn\ s}{m^2} = 0.1\ Pa\ s$. From the table one can see that the viscosity of water is 1.79 x 10^{-2} poise at 0° which falls to 2.838x10^{-3} poise at 100°. For comparison, the viscosity of air at 20° is 181 x 10^{-6} poise and the viscosities of lubricating oils are typically 1-10 poise.

8. SUPPLEMENTAL QUESTIONS

Each of the magnetic moments in a sample is influenced by the magnetic fields of other moments in its neighborhood. These differ from location to location in the sample, depending on the relative distance and orientation of neighbor moments to one another. An approximate measure of the magnetic field variation experienced by the proton moments in the water molecule is the range corresponding to parallel alignment of two interacting protons at one extreme to opposite alignment at the other.

1. Using μ/r^3 for the field of the neighbor moment, show that the half-range in the Larmor precession frequencies is given by $\Delta\omega \approx (g\mu_n)^2/hr^3$.

2. The return to normal of the transverse distribution of the protons following resonance occurs as moments with different precession frequencies become more and more randomly orientated in the precession angle. Estimate the transverse relaxation time T_2 for the water sample by finding the time required for two moments, differing by the average $\Delta\omega$ calculated in part a., to move from in-phase to π-out-of-phase positions.

As you've probably guessed, this lab is merely a stepping off point for an incredibly varied set of potential investigations. Some good general references for this lab (beyond the ones already cited in the text) are [13–19].

[1] F. Bloch, Phys. Rev. **70**, 460 (1946).
[2] N. Bloembergen, E. Purcell, and R. Pound, Phys. Rev. **73**, 679 (1948).
[3] *Nobel Lecture for Felix Bloch and Edward Mills Purcell* (1952).
[4] A. Abragam, *Principles of Nuclear Magnetism* (Oxford University Press, 1961), ISBN QC762.A158, physics Department Reading Room.
[5] Derome, Mod. NMR Technique. For Chem. Research (1987).
[6] E. Hahn, Phys.Rev. **80**, 580 (1950).
[7] E. Hahn, Phys Today **Nov. 1953**, 4 (1953).
[8] H. Carr and E. Purcell, Phys. Rev **94**, 630 (1954).
[9] S. Meiboom and D. Gill, Rev. Sci. Inst. **29**, 668 (1958), a short paper with a major modification of the Carr-Purcell sequence. Without such a modification, it is not possible to generate a long train of echoes. This is an early application of a complex multiple-pulse sequence with phase shifts which have become routine.
[10] I. Chuang, Junior Lab Paper (1990).
[11] R. Ernst and W. Anderson, Rev. Sci. Instrum. **37**, 93 (1966).
[12] N. Bloembergen, *Nuclear Magnetic Relaxation* (W.A. Benjamin, 1961), ISBN QC173.B652, physics Department Reading Room.
[13] G. Pake, American Journal of Physics **18**, 438 (1950).
[14] T. Farrar and E. Becker, *Pulse and FT NMR* (Acad. Press, 1971), ISBN QC454.F244, physics Department Reading Room.
[15] Feynman, Leighton, and Sands, *Lectures on Physics*, vol. Volume II, Chapter 35 (Addison-Wesley, 1965), ISBN QC23.F435, interesting discussions of angular momentum, the Stern-Gerlach Experiment and NMR, Physics Department Reading Room.
[16] E. Fukushima and S. Roeder, *Experimental Pulse NMR* (Addison-Wesley, 1981), ISBN QC762.F85, an excellent practical reference, Science Library Stacks.
[17] R. Freeman, *A Handbook of Nuclear Magnetic Resonance*

(Farragut Press, 1997), 2nd ed., ISBN QD96.N8.F74, spin-Lattice Relaxation, Science Library Stacks.
[18] G. Pake, Annual Review of Nuclear Science **19**, 33 (1954).
[19] G. Pake, Sci. Amer. **Aug.** (1958), an excellent introduction, Science Library Journal Collection.

Appendix A: Quantum Mechanical Description of NMR

Recall that for all spin-1/2 particles (protons, neutrons, electrons, quarks, leptons), there are just two eigenstates, spin up: $|S, S_z\rangle = |\frac{1}{2}, \frac{1}{2}\rangle \rightarrow |0\rangle$ and spin down: $|S, S_z\rangle = |\frac{1}{2}, \frac{-1}{2}\rangle \rightarrow |1\rangle$. Using these as basis vectors, the general state of a spin-1/2 particle can be expressed as a two-element column matrix called a **spinor**:

$$|\psi\rangle = u|0\rangle + d|1\rangle = \begin{bmatrix} u \\ d \end{bmatrix}. \tag{A1}$$

Normalization imposes the constraint $|u|^2 + |d|^2 = 1$.

The system is governed by the Schrödinger equation:

$$i\hbar \frac{d}{dt}|\psi\rangle = H|\psi\rangle \tag{A2}$$

which has the solution $|\psi(t)\rangle = U|\psi(0)\rangle$, where $U = e^{-iHt/\hbar}$ is unitary. In pulsed NMR, the Hamiltonian

$$H = -\vec{\mu} \cdot \vec{B} = -\mu[\sigma_x B_x + \sigma_y B_y + \sigma_z B_z] \tag{A3}$$

is the potential energy of a magnetic moment placed in an external magnetic field. The σ's are the Pauli spin matrices,

$$\sigma_x \equiv \begin{bmatrix} 0 & 1 \\ 1 & 0 \end{bmatrix}, \quad \sigma_y \equiv \begin{bmatrix} 0 & -i \\ i & 0 \end{bmatrix}, \quad \sigma_z \equiv \begin{bmatrix} 1 & 0 \\ 0 & -1 \end{bmatrix}. \tag{A4}$$

Inserting (A4),(A1) and (A3) into (A2), we get:

$$\dot{u} = \mu\left[iB_x + B_y\right] d + i\mu B_z u \tag{A5}$$

$$\dot{d} = \mu\left[iB_x - B_y\right] u - i\mu B_z d \tag{A6}$$

If $B_x = B_y = 0$ and the equations reduce to

$$\dot{u} = i\mu B_z u, \quad \dot{d} = -i\mu B_z d. \tag{A7}$$

Integrating with respect to time yields

$$u = u_0 e^{i\mu B_z t} = u_0 e^{i\omega_0 t}, \quad d = d_0 e^{-i\mu B_z t} = d_0 e^{-i\omega_0 t} \tag{A8}$$

where $\omega_0 = \mu B_z/\hbar$ is the **Larmor Precession Frequency**. If an atom undergoes a spin-flip transition from the 'spin-up' state to the 'spin-down' state, the emitted photon has energy $E = 2\omega_0\hbar$.

Now let's add a small external magnetic field B_x but still keeping $B_y = 0$ and such that $B_x \ll B_z$. Equations A5 and A6 become:

$$\dot{u} = i\mu B_x d/\hbar - i\mu B_z u/\hbar \tag{A9}$$

$$\dot{d} = i\mu B_x u/\hbar + i\mu B_z d/\hbar \tag{A10}$$

For a time varying magnetic field of the type produced by an 'RF-Burst' as in pulsed NMR, $B_x = B_{x0}\cos\omega t = B_{x0}\left(e^{i\omega t} + e^{-i\omega t}\right)/2$. Define $\omega_x = \mu B_x/\hbar$. We see that

$$\dot{u} = -i\omega_0 u + i\omega_x\left(e^{i\omega t} + e^{-i\omega t}\right) d/2 \tag{A11}$$

$$\dot{d} = i\omega_0 d + i\omega_x\left(e^{i\omega t} + e^{-i\omega t}\right) u/2 \tag{A12}$$

Using $\omega_x \ll \omega_0$ since $B_x \ll B_0$, we can try for a solution of the form

$$u = C_u(t)e^{-i\omega_0 t}, \quad d = C_d(t)e^{i\omega_0 t} \tag{A13}$$

Inserting them into the differential equations for u and d, we get

$$\dot{C_u} = \frac{i\omega_x}{2} C_d\left[e^{i(\omega-2\omega_0)t} + e^{-i(\omega-2\omega_0)t}\right] \tag{A14}$$

$$\dot{C_d} = \frac{i\omega_x}{2} C_u\left[e^{i(\omega-2\omega_0)t} + e^{-i(\omega+2\omega_0)t}\right] \tag{A15}$$

Now we use the approximation $\omega \ll \omega_0$ to show that the leading terms are very small. If we run at **resonance** ($\omega = 2\omega_0$):

$$\dot{C_u} = \frac{i\omega_x}{2} C_d, \quad \dot{C_d} = \frac{i\omega_x}{2} C_u \tag{A16}$$

Taking the derivatives of these equations, we see that these coefficients act like harmonic oscillators of frequency $\omega_x/2$. These have the general solution

$$C_u = a\cos\left(\omega_x t/2\right) + b\sin\left(\omega_x t/2\right) \tag{A17}$$

$$C_d = ia\sin\left(\omega_x t/2\right) - ib\cos\left(\omega_x t/2\right) \tag{A18}$$

Putting these in A13, we get the solution for u and d. These are called **Rabi Oscillations**, valid for $\omega_x \ll \omega_0$.

Appendix B: Bloch Sphere Representation

A single qubit in the state $a|0\rangle + b|1\rangle$ can be visualized as a point (θ, ϕ) on the unit sphere, where $a = \cos(\theta/2)$, $b = e^{i\phi}\sin(\theta/2)$, and a can be taken to be real because the overall phase of the state is unobservable. This is called the Bloch sphere representation, and the vector $(\cos\phi\sin\theta, \sin\phi\sin\theta, \cos\theta)$ is called the Bloch vector.

The Pauli matrices give rise to three useful classes of unitary matrices when they are exponentiated, the *rotation operators* about the $\hat{x}$, $\hat{y}$, and $\hat{z}$ axes, defined by the

equations:

$$R_x(\theta) \equiv e^{-i\theta X/2} = \cos\frac{\theta}{2}I - i\sin\frac{\theta}{2}X = \begin{bmatrix} \cos\frac{\theta}{2} & -i\sin\frac{\theta}{2} \\ -i\sin\frac{\theta}{2} & \cos\frac{\theta}{2} \end{bmatrix} \quad \text{(B1)}$$

$$R_y(\theta) \equiv e^{-i\theta Y/2} = \cos\frac{\theta}{2}I - i\sin\frac{\theta}{2}Y = \begin{bmatrix} \cos\frac{\theta}{2} & -\sin\frac{\theta}{2} \\ \sin\frac{\theta}{2} & \cos\frac{\theta}{2} \end{bmatrix} \quad \text{(B2)}$$

$$R_z(\theta) \equiv e^{-i\theta Z/2} = \cos\frac{\theta}{2}I - i\sin\frac{\theta}{2}Z = \begin{bmatrix} e^{-i\theta/2} & 0 \\ 0 & e^{i\theta/2} \end{bmatrix}. \quad \text{(B3)}$$

One reason why the $R_{\hat{n}}(\theta)$ operators are referred to as rotation operators is the following fact. Suppose a single qubit has a state represented by the Bloch vector $\vec{\lambda}$. Then the effect of the rotation $R_{\hat{n}}(\theta)$ on the state is to rotate it by an angle θ about the $\hat{n}$ axis of the Bloch sphere.

An arbitrary unitary operator on a single qubit can be written in many ways as a combination of rotations, together with global phase shifts on the qubit. A useful theorem to remember is the following: Suppose U is a unitary operation on a single qubit. Then there exist real numbers α, β, γ and δ such that

$$U = e^{i\alpha}R_x(\beta)R_y(\gamma)R_x(\delta)\,. \quad \text{(B4)}$$

Appendix C: Fundamental equations of magnetic resonance

The magnetic interaction of a classical electromagnetic field with a two-state spin is described by the Hamiltonian $H = -\vec{\mu}\cdot\vec{B}$, where $\vec{\mu}$ is the spin, and $B = B_0\hat{z} + B_1(\hat{x}\cos\omega t + \hat{y}\sin\omega t)$ is a typical applied magnetic field. B_0 is static and very large, and B_1 is usually time varying and several orders of magnitude smaller than B_0 in strength, so that perturbation theory is traditionally employed to study this system. However, the Schrödinger equation for this system can be solved straightforwardly without perturbation theory, in terms of which the Hamiltonian can be written as

$$H = \frac{\omega_0}{2}Z + g(X\cos\omega t + Y\sin\omega t)\,, \quad \text{(C1)}$$

where g is related to the strength of the B_1 field, and ω_0 to B_0, and X, Y, Z are the Pauli matrices as usual. Define $|\phi(t)\rangle = e^{i\omega tZ/2}|\chi(t)\rangle$, such that the Schrödinger equation

$$i\partial_t|\chi(t)\rangle = H|\chi(t)\rangle \quad \text{(C2)}$$

can be re-expressed as

$$i\partial_t|\phi(t)\rangle = \left[e^{i\omega Zt/2}He^{-i\omega Zt/2} - \frac{\omega}{2}Z\right]|\phi(t)\rangle\,. \quad \text{(C3)}$$

Since

$$e^{i\omega Zt/2}Xe^{-i\omega Zt/2} = (X\cos\omega t - Y\sin\omega t)\,, \quad \text{(C4)}$$

(C3) simplifies to become

$$i\partial_t|\phi(t)\rangle = \left[\frac{\omega_0-\omega}{2}Z + gX\right]|\phi(t)\rangle\,, \quad \text{(C5)}$$

where the terms on the right multiplying the state can be identified as the effective 'rotating frame' Hamiltonian. The solution to this equation is

$$|\phi(t)\rangle = e^{i\left[\frac{\omega_0-\omega}{2}Z+gX\right]t}|\phi(0)\rangle\,. \quad \text{(C6)}$$

The concept of *resonance* arises from the behavior of this solution, which can be understood to be a single qubit rotation about the axis

$$\hat{n} = \frac{\hat{z} + \frac{2g}{\omega_0-\omega}\hat{x}}{\sqrt{1+\left(\frac{2g}{\omega_0-\omega}\right)^2}} \quad \text{(C7)}$$

by an angle

$$|\vec{n}| = t\sqrt{\left(\frac{\omega_0-\omega}{2}\right)^2 + g^2}\,. \quad \text{(C8)}$$

When ω is far from ω_0, the spin is negligibly affected by the B_1 field; the axis of its rotation is nearly parallel with $\hat{z}$, and its time evolution is nearly exactly that of the free B_0 Hamiltonian. On the other hand, when $\omega_0 \approx \omega$, the B_0 contribution becomes negligible, and a small B_1 field can cause large changes in the state, corresponding to rotations about the $\hat{x}$ axis. The enormous effect a small perturbation can have on the spin system, when tuned to the appropriate frequency, is responsible for the 'resonance' in nuclear magnetic resonance.

In general, when $\omega = \omega_0$, the single spin rotating frame Hamiltonian can be written as

$$H = g_1(t)X + g_2(t)Y\,, \quad \text{(C9)}$$

where g_1 and g_2 are functions of the applied transverse RF fields.

Appendix D: Modeling the NMR Probe

The material in this appendix was provided by Professor Isaac Chuang. A tuned circuit is typically used to efficiently irradiate a sample with electromagnetic fields in the radiofrequency of microwave regime. This circuit allows power to be transferred from a source with minimal reflection, while at the same time creating a large electric of magnetic field around the sample, which is typically placed within a coil that is part of it.

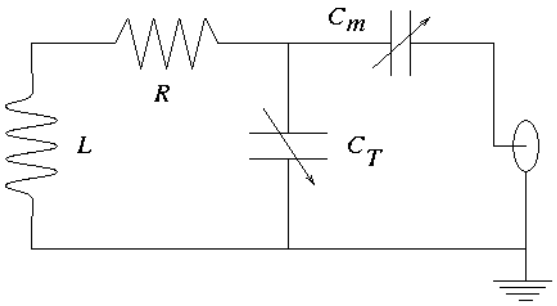

FIG. 9: Schematatic diagram of NMR probe circuit. The connector on the right goes off to the source and any detection circuitry.

1. Circuit and Input Impedance

A typical probe circuit, as shown in Figure 7, consists of an inductor L, its parasitic coil resistance R, a tuning capacitor C_T, and an impedance matching capacitor C_m. We can analyze the behavior of this circuit using the method of complex impedances, in which the capacitors have impedance $Z_C = 1/i\omega C$, inductors $Z_L = i\omega L$, and resistors $Z_R = R$, with $\omega = 2\pi f$ being the frequency in rad/sec. The input impedance is thus

$$\begin{aligned} Z &= Z_{C_m} + \left[\frac{1}{Z_{C_T}} + \frac{1}{R + Z_L}\right]^{-1} \\ &= \frac{1}{i\omega C_m} + \left[i\omega C_T + \frac{1}{R + i\omega L}\right]^{-1} \\ &= \frac{1 + i\omega R(C_T + C_m) - \omega^2 L(C_T + C_m)}{i\omega C_m(1 + iR\omega C_T - \omega^2 L C_T)}. \end{aligned} \quad \text{(D1)}$$

2. Tune and Match Conditions

The resonant frequency of this circuit is set by

$$\omega_*^2 = \frac{1}{L(C_T + C_m)}\,, \quad \text{(D2)}$$

and at this frequency, the input impedance is

$$Z_0 = \frac{R(C_T + C_m)}{C_m(1 + iR\omega_* C_T - \omega_*^2 L C_T)}\,. \quad \text{(D3)}$$

We would like this impedance to be 50 ohms, because that is the typical impedance expected by RF or microwave sources and the coaxial cable which carries in the signal. Setting $Z_0 = 50$ we obtain:

$$\frac{50}{R} = \frac{(C_T + C_m)^2}{C_m\left[C_m + iR\omega_* C_T(C_T + C_m)\right]}. \quad \text{(D4)}$$

To good approximation, the $iR\omega_* C_T(C_T + C_m)$ term in the denominator may be neglected, giving

$$\frac{50}{R} = \left(1 + \frac{C_T}{C_m}\right)^2. \quad \text{(D5)}$$

When these conditions are satisfied, almost all the source power goes into the tuned resonator at the resonant frequency, thus creating the strongest possible oscillating magnetic field inside the coil L.